2021 43rd Annual International Conference of the
IEEE Engineering in Medicine & Biology Society (EMBC)
Oct 31 - Nov 4, 2021. Virtual Conference

Laser Power Determination Using Light-to-Heat Conversion Rate of Nanoplasmonic Substrates for Neural Stimulation

Yujin An, and Yoonkey Nam, *Member, IEEE*

***Abstract*— Since neurons have temperature sensitive properties, gold nanorod (GNR)-mediated photothermal stimulation has been developed as a neuromodulation application. As an *in vitro* photothermal platform, GNR-layer was integrated with substrates to effectively apply heat stimulation to the cultured neurons. However, identifying optimal laser power for a targeted temperature on the substrate requires the consideration of thermal properties of the GNR-coated substrates. In this report, we suggest a simple numerical method to determine incident laser power on the substrates for a targeted temperature.**

I. Introduction

Photothermal stimulation is a promising technology for neuromodulation. By controlling light, neuronal activity is excited [1] or inhibited [2] by heat that is converted from absorbed light energy by materials. For this technology, temperature is a crucial factor to determine neural responses because of temperature-sensitive properties of tissues. However, accurate measurement of temperature during photothermal stimulation is challenging due to the limitation of thermal imaging at depth in tissue and artifacts of thermocouples induced by light absorption.

As a platform of photothermal neural stimulation, substrates coated with metallic nanoparticle have been developed. Thermoplasmonic effect of metallic nanoparticles effectively induces heat upon light. Tuning a resonant wavelength of metallic nanoparticles at near infrared (NIR) light allows generating heat only on the surface of the substrate due to the low NIR light absorption of water. The examples of photothermal neural stimulation substrates include multielectrode arrays (MEA) [3] or optical fiber [4] integrated with gold nanorods (GNRs) or gold nanostars [5], or a gold nanofilm [6] for neural stimulation. For the various forms of substrates, proper neural stimulation requires a method to identify an optimal laser power for a targeted temperature. Due to the difficulty of temperature measurement during photothermal stimulation, we suggest a simple computation modeling to estimate the maximal temperature upon light and determine laser power on the substrates.

For the photothermal substrate integrated with nanoparticles, characterizing its light-to-heat conversion rate is required. In fact, heat conversion efficiency varies greatly depending on the shape [7], size [8], and concentration [9] of the metallic particles. In addition, with identical nanoparticles, the substrates may have a different degree of efficiency owing to different adhesion. Therefore, direct measurement of light-to-heat efficiency of the substrates is required. For example, other studies measured absorbance of substrates with a plasmonic layer to characterize its light-to-heat conversion efficiency [4], [10], [11]. However, in order to make heat conversion process of substrates clear, it is necessary to directly measure the temperature increase upon light illumination.

In this work, we suggest a simple numerical method to determine an optimal laser power for a targeted temperature on photothermal substrates (Figure 1A). Here, GNR-coated MEA chips were used as the substrates (Figure 1B). To measure light-thermal conversion rates (CR) of GNR-coated MEA chips, we measured temperature increase of those upon light illumination (Figure 1C). To identify the relationship between the temperature rises on the neuron culture substrates and applied heat power, we derived thermal resistances of the photothermal stimulation condition from a numerical heat transfer simulation.

II. Materials and Methods

A. GNR synthesis and GNR coating on MEA

Seed-mediated methods were used to synthesize gold nanorods (GNRs), which were then coated with Thiol-PEG-

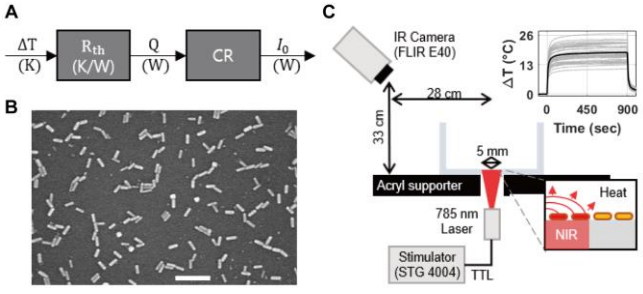

Figure 1. **A.** Overview of laser power determination for a target maximal temperature increase on the GNR-coated MEA. **B.** Gold-nanorods integrated on the substrate. (bar: 200 nm). **C.** The measurement of light-to-heat conversion rate (CR) of each MEA chip. Maximal temperature increase of the MEA surface upon NIR light is also shown.

* This work was supported by National Research Foundation grants (NRF-2021R1A2B5B03001764, NRF-2018R1A2A1A05022604) funded by Korean government.

Y. An, and Y. Nam are with the Department of Bio and Brain Engineering, KAIST, Daejeon, 34141 Republic of Korea (e-mail: elrlemrm@kaist.ac.kr, ynam@kaist.ac.kr, respectively).

Amine (HS-PEG-NH2, Laysan Bio) [3]. The synthesized GNRs had the maximal absorption peak at the wavelength of 783 nm and +7.24 mV of zeta potential. Next, GNRs were uniformly attached on glass substrate MEA (Multi Channel Systems, Reutlingen, Germany) [3]. For this, the MEA chip was treated with 70 W plasma for 1 min and loaded 500 μL GNR solution (1 OD). The MEA chip was stored in humid incubator for 12 hours.

B. Definition of light-to-heat conversion rate (CR) of GNR-coated MEA and its measurement

When GNR-coated MEA is illuminated with NIR light, temperature increase (ΔT) at steady-state can be represented by multiplication of heat (Q) and heat resistance (R_{th}) of the condition.

$$\begin{aligned}\Delta T[K] &= Q_{total}\,[W] \times R_{th}\,[K/W] \\ &= (Q_{MEA} + Q_{GNR}) \times R_{th} \\ &= I_0 \times (A_{MEA} \cdot \eta_{MEA} + T_{MEA} \cdot A_{GNR} \cdot \eta_{GNR}) \times R_{th}\end{aligned} \quad (1)$$

where, Q_{MEA} is the heat generated from MEA upon NIR illumination regardless of the existence of GNR, Q_{GNR} is the heat generated from GNRs on the MEA surface, A is absorbance of a MEA substrate or GNR-layer, η is conversion rate from absorbed light energy to thermal energy, T_{MEA} is a fraction of light transmitting the glass substrate of the MEA. R_{th} changes according to materials and diameters of heat sources on the surface of MEA. The value of R_{th} was calculated by using a heat transfer simulation or a temperature profile equation (equation 4) when 2D nano-heat sources were uniformly distributed on the boundary surface of two materials.

Based on equation 1, CR was defined as the rate of thermal energy to incident light energy on the MEA.

$$CR = A_{MEA} \times \eta_{MEA} + T_{MEA} \times A_{GNR} \times \eta_{GNR} \quad (2)$$

which means that the total amount of heat consists of the heat generated from a MEA substrate itself and the heat that is converted from the light passing through the MEA substrate and absorbed by GNRs. CR allows us to estimate a heat flux (W/m^2) for an incident laser density (W/m^2) applied to MEA surface.

To measure CR of the GNR-coated MEA, a constant power of NIR laser (diameter = 5 mm, 429 mW, 785 nm) was illuminated on the MEA in air and the maximal temperature increase of the illuminated area at steady-state was measured with an IR camera (FLIR E40). Next, CR was calculated as follows:

$$CR = \frac{\Delta T\,[K]}{I_0\,[W] \times R_{th}\left[\frac{K}{W}\right]}, \quad (3)$$

where, R_{th} is the thermal resistance (218.33 K/W) on the heat sources of 5 mm diameter. R_{th} for this condition was derived from a COMSOL heat transfer simulation (Figure 2A) as described on the next section.

C. Simulation for thermal resistance

To identify thermal resistances on the GNR-coated MEA in two different cases, finite-element method (FEM) models were constructed using COMSOL Multiphysics 5.5 (COMSOL Inc., Burlington MA, USA) as shown in Figure2. We created 2D axisymmetric models that were the same as the dimension of the MEA chip. The materials of these models are described in Table 1. The heat was generated at the central boundary region of the models (blue line pointed with a blue arrow). Convection conditions were applied to all boundary (convective coefficient = 10 $W/(m^2 \cdot K)$) and a room temperature of 24 ℃. Meshs were set as extra fine, and the domains near the z-axis (Figure 2A, r = 2.5 mm; Figure 2C, r = 4 mm) had a maximum element size of 50 μm. The time step was 0.1 sec.

Figure 2A shows the model of the MEA chip in air. The number of elements and nodes were 2869 and 1555, respectively. To validate this model, the temperature dynamics measured on the center of the MEA chip upon NIR illumination was compared with the calculated one in the simulation (Figure 2B). Figure 2C shows a model for the condition of photothermal neural stimulation, which was constructed to identify the thermal resistance. The number of elements and nodes were 18743 and 10196, respectively. The MEA chip had liquid media with 1 mL and a Teflon ring. The convection of water and air was set as weakly compressible fluids. A constant temperature (37 ℃) was applied to the bottom surface imitating the experimental condition. The inner wall condition of the fluid was applied to the interface between water and air with a fluid velocity of zero.

Thermal resistance R_{th} for each condition was derived from the slope of temperature increases at the center of the MEA chip for four different heat fluxes.

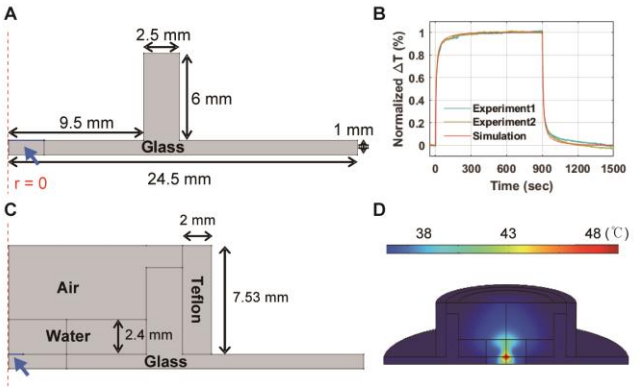

Figure 2. Heat transfer simulation to calculate thermal resistance of MEA chips. 2D axisymmetric model for the MEA chip was built using COMSOL Multiphysics software. **A.** A model for the MEA chip in air. The blue line (radius = 2.5 mm) is a heat source. **B.** Overlapped temperature data of simulation in Figure A and measurement of MEA chip is shown. **C.** A model for the MEA chip in which neurons are cultured. The heat source (blue line) of 1 mm radius is represented. **D**. With the model in Figure C, 3D temperature distribution at 300 sec with heat flux density of 25 mW/mm^2.

TABLE I. THERMAL PROPERTIES OF MATERIALS APPLIED TO THE GNR-COATED MEA SIMULATIONS.

	Density kg/m^3	Heat capacity $J/(kg \cdot K)$	Thermal conductivity $W/(m \cdot K)$
Glass	2210	730	1.4
Teflon	2136	1002	0.273
Air	1.138	1006	0.027
Water	993.23	4189	0.625

All values were provided by COMSOL Multiphysics 5.5. The table shows the average of material properties at the baseline temperature (37 ℃).

D. *Estimation of maximal temperature depending on the size of laser spot and CR*

With a uniformly distributed heat source density (W/m^2) with a circular shape on the boundary surface between air and the MEA chip (glass), a steady-sate temperature rise on the center of the heat source (ΔT) was calculated as follows[12]:

$$\Delta T = \frac{q_0}{2k} R = \frac{1}{\pi \cdot k \cdot D} Q, \quad (4)$$

here, q_0 is the two-dimensional heat density (W/m^2) uniformly distributed over space, R is the radius and diameter of heat source (m), k (1.013 W/(K·m)) is the average of thermal conductivities of glass and water, and Q is power (W) of the heat source, D (m) is the diameter of the heat source. The thermal resistance $R_{th} = 1/(\pi \cdot k \cdot D)$ in this formula was validated by using COMSOL heat transfer simulation. Given a diameter of light source, the simulation calculated the temperature increases on the center of the MEA chip at steady-state upon four different heat power. The thermal resistances for each light diameter was obtained from the slope of linear regression lines for the temperature increase points.

We determined the input laser power that is required to make a targeted temperature increase (ΔT^*) as follows:

$$I\,[W] = \frac{\Delta T^* \cdot R_{th}}{CR} = \frac{\Delta T^* \cdot (1/k \cdot \pi \cdot D)}{CR}, \quad (5)$$

E. *Measurement of absorbance of GNRs-layer*

The absorbance of the GNR-layer on the MEA chip (A_{GNR}) was measured by using a spectrometer and a power meter. We figured the ratio of the light absorbed into the GNR-layer, after transmitting the bare MEA chip, to the incident light. It was calculated by subtracting the transmittance of the bare MEA chip with the transmittance of the GNRs-coated MEA chip.

$$T_{MEA} - T_{MEA} \times T_{GNR} = T_{MEA} \times (1 - T_{GNR}) = T_{MEA} \times A_{GNR} \quad (6)$$

where, scattering of GNR was ignored.

To measure the transmittance of the MEA chip, OceanView software (Ocean Optics Inc.) was utilized. A halogen light source (HL-2000, Ocrean Optics) was used as a light source. An aperture with a hole of 1 mm diameter at the center of it put above the light sources, and then the MEA chip was placed on the center of the aperture. A spectrometer (USB4000-VIS-NIR-ES, Ocean Optics) was installed 3 cm above the bottom surface of the MEA. The transmittance of the MEA chips (n = 8 chips) at 785 nm wavelengths was measured before and after the GNR coating.

To measure the laser power, a laser light (spot size: 5 mm in diameter, 785 nm, max 450 mW, B&W Tek) was illuminated on the MEA surface with the density of 21.9 mW/mm^2. The intensity of the light was measured for 30 seconds with a power meter (XLP12-3S-H2, Gentec-EO, CA). The measurements were averaged to calculate the transmittance of MEA chips (n = 8) before and after the GNR coating.

III. Result

A. *Measurement of CR for GNR-coated MEA chips*

Figure 3A shows the measurement of CRs of GNR-coated MEA chips. Despite the same GNR coating protocol, CRs of each MEA chip was significant different, indicating some variation of MEA surface coverage. The distribution of CR had a mean of 0.20 and a standard deviation of 0.04 when fitted as a normal distribution.

B. *Validation of CR by comparing with absorbance of GNR-coated MEA chips*

We validated CR by comparing an optical property of the GNR-coated MEA chips. We measured the absorbance of the GNR-layer on the MEAs ($T_{MEA} \times A_{GNR}$), which considered the light absorbed by the GNRs-layer and the MEA substrate. Comparing the absorbance measured by a spectrometer to the calculated CR, we found that CRs were correlated with the absorbance of the GNRs-layer (slope = 1.057 R^2 =0.929) as shown in Figure 3B. In addition, although the absorbance by the GNR layer was zero, the CR had a value of about 0.035, which means the heat generated by the MEA chip itself. This trend was also identified with the measurement using a power meter (slope = 1.187, R^2=0.947, y-intercept = 0.029; data not shown). The slope of the graph represents η_{GNR} in the equation 2. The value of η_{GNR} in this experiment was consistent with the reported photothermal efficiency (~ 1) of the GNR [13].

C. *The thermal resistance of the MEA chip and its validation*

We calculated the thermal resistance of the MEA chip on the condition of photothermal stimulation by using the equation 4 and the simulation model in Figure 2C. Table 2 shows the summarized results. In the theoretical calculation, as the diameters of laser spots were reduced, the thermal resistances increased, which means that a smaller diameter induces a higher temperature increase upon the same laser power. The thermal resistances extracted from the FEM model (Figure 2C) were nearly identical with those from equation 4, indicating that GNR-layer case can be approximated by the equation 4.

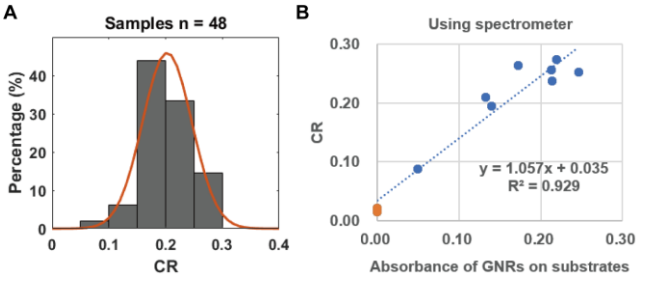

Figure 3. Measurement of CR and absorbance of GNR-coated MEA chip. **A.** The distribution of CR for GNR-coated MEA chips. **B.** Relationship between absorbance of GNR-coated substrates and CR. Orange dots represent data of bare MEA chips.

TABLE II. THERMAL RESISTANCES DEPENDING ON LIGHT DIAMETERS.

Thermal resistance R_{th}	Light diameter (mm)				
	2.0	**1.6**	**1.0**	**0.5**	**0.2**
Calculation	157	196	314	628	1571
Simulation	166	208	332	656	1593

D. Determination of Input laser power for a target temperature

To calculate laser power for a targeted temperature rise on thermoplasmonic substrates for the condition of photothermal neural stimulation, we used equation 5 with the consideration of the measured CRs and the diameters of the incident laser spots on the MEA surfaces. Figure 4 shows that an increase in CR from 0.09 to 0.29 led to a decrease in input laser power from 726 mW to 221 mW for 2 mm diameter. This means that the CR of the MEA chip plays a significant role in determination of the incident laser power required for a target temperature. Furthermore, by reducing the size of the laser spot 10 times (D = 0.2 mm), we can drop the laser power 10 times for the target maximum temperature.

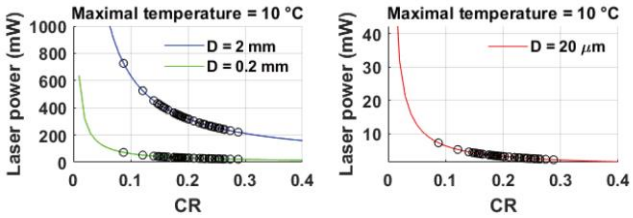

Figure 4. Incident laser power to obtain a targeted maximal temperature increase (10 °C) on the MEA chip. The black circles indicate the input laser power corresponding to the measured CR for. The solid lines represent different sizes of laser spots and its required laser power for the targeted temperature rise in range of all CRs.

IV. DISCUSSION

The advantage of our method is that the range of laser power of photothermal neural stimulation on a substrate can be determined through a simple calculation. Studies reported neural silence was induced by temperature increase ranged from 8 to 13 °C with the baseline temperature of 37 °C [3]. In the previous study, the laser power ranged from 1 to 10 mW needed for the localized photothermal stimulation with a laser spot (diameter = 20 um, wavelength = 785 nm) to suppress neural activity on the GNR-coated MEA chip [14]. At 10 mW of laser power, neuronal activities were completely inhibited. At 19 mW of laser power, irreversible neuronal activity was caused. The range of laser power from our computational method corresponded to that in the experimental results of the localized photothermal stimulation. Figure 4 shows that the range from 2.2 to 7.2 mW of laser power was required for the temperature increase of 10 °C with the laser diameter of 20 um. In addition, more than three times the laser power in this range appears to be capable of damaging neurons. Therefore, our computational method can simply find out the range of laser inputs that can safely stimulate neurons on thermoplasmonic substrates.

V. CONCLUSION

In summary, we presented a simple method by using a thermal resistance equation at steady-state in order to estimate the maximal temperature increase induced by light on thermoplasmonic substrates. First, light-to-heat conversion rate of the thermoplasmonic substrates was determined by measuring the temperature increase when the same laser power was applied to each substrate. It was confirmed that heat conversion rates were different even with the same fabrication process for the substrates. This measured heat conversion rate was correlated with the amount of light absorbed from the thermal plasmonic layer on the substrate. As a result, the consideration of heat conversion rate of thermoplasmonic substrates enabled us to properly determine input laser power for photothermal neural stimulation.

REFERENCES

[1] K. Eom *et al.*, "Enhanced Infrared Neural Stimulation using Localized Surface Plasmon Resonance of Gold Nanorods," *Small*, vol. 10, no. 19, pp. 3853–3857, 2014.

[2] S. Yoo, S. Hong, Y. Choi, J. H. Park, and Y. Nam, "Photothermal inhibition of neural activity with near-infrared-sensitive nanotransducers," *ACS Nano*, vol. 8, no. 8, pp. 8040–8049, 2014.

[3] S. Yoo, R. Kim, J. H. Park, and Y. Nam, "Electro-optical Neural Platform Integrated with Nanoplasmonic Inhibition Interface," *ACS Nano*, vol. 10, no. 4, pp. 4274–4281, 2016.

[4] H. Kang, W. Hong, Y. An, S. Yoo, H. J. Kwon, and Y. Nam, "Thermoplasmonic Optical Fiber for Localized Neural Stimulation," *ACS Nano*, vol. 14, no. 9, pp. 11406–11419, 2020.

[5] J. W. Lee, H. Jung, H. H. Cho, J. H. Lee, and Y. Nam, "Gold nanostar-mediated neural activity control using plasmonic photothermal effects," *Biomaterials*, vol. 153, pp. 59–69, 2018.

[6] J. W. Lee, H. Kang, and Y. Nam, "Thermo-plasmonic gold nanofilms for simple and mass-producible photothermal neural interfaces," *Nanoscale*, vol. 10, no. 19, pp. 9226–9235, 2018.

[7] V. P. Pattani and J. W. Tunnell, "Nanoparticle-mediated photothermal therapy: A comparative study of heating for different particle types," *Lasers Surg. Med.*, vol. 44, no. 8, pp. 675–684, 2012.

[8] K. Jiang, D. A. Smith, and A. Pinchuk, "Size-dependent photothermal conversion efficiencies of plasmonically heated gold nanoparticles," *J. Phys. Chem. C*, vol. 117, no. 51, pp. 27073–27080, 2013.

[9] H. Zhang, H. J. Chen, X. Du, and D. Wen, "Photothermal conversion characteristics of gold nanoparticle dispersions," *Sol. Energy*, vol. 100, pp. 141–147, 2014.

[10] Y. Lee *et al.*, "Nanoplasmonic On-Chip PCR for Rapid Precision Molecular Diagnostics," *ACS Appl. Mater. Interfaces*, vol. 12, no. 11, pp. 12533–12540, 2020.

[11] S. Principe *et al.*, "Thermo-plasmonic lab-on-fiber optrodes," *Opt. Laser Technol.*, vol. 132, no. April, pp. 1–10, 2020.

[12] G. Baffou, "Two-Dimentional Heat Sources," in *Thermoplasmonics: Heating Metal Nanoparticles Using Light*, 2018, p. 55.

[13] Z. Qin *et al.*, "Quantitative comparison of photothermal heat generation between gold nanospheres and nanorods," *Sci. Rep.*, vol. 6, no. April, pp. 1–13, 2016.

[14] S. Yoo, J.-H. Park, and Y. Nam, "Single-Cell Photothermal Neuromodulation for Functional Mapping of Neural Networks," *ACS Nano*, vol. 13, p. acsnano.8b07277, 2019.